Nanoscale

PAPER

View Article Online
View Journal | View Issue

Cite this: *Nanoscale*, 2015, **7**, 18998

Rapid and selective detection of viruses using virus-imprinted polymer films

A. Karthik,[a] K. Margulis,[a] K. Ren,[a,b] R. N. Zare*[a] and L. W. Leung[c]

Received 6th September 2015,
Accepted 15th October 2015

DOI: 10.1039/c5nr06114h

www.rsc.org/nanoscale

We prepared a nanopatterned polymer film of polydimethylsiloxane (PDMS) *via* virus imprinting. The imprinted surface exhibited nanoscale cavities with the mean size of 120 ± 4 nm. These cavities demonstrated the ability to preferentially capture a target virus from an aqueous suspension of ultralow volume (5 μL) after only 1 minute of contact. Two inactivated viruses with similar shape, Influenza A (HK68) and Newcastle Disease Virus (NDV), were employed as model pathogens. The polymer film, which was first imprinted with HK68 and exposed sequentially to suspensions containing fluorescently labeled NDV and HK68, was able to preferentially bind HK68 at a capture ratio of 1 : 8.0. When we reversed the procedure and imprinted with NDV, the capture ratio was 1 : 7.6. These results were obtained within 20 minutes of static exposure. The suspensions contained viruses at concentrations close to those occurring physiologically in influenza infections. The limit of detection was approximately 8 fM. Production of virus-imprinted films can be readily scaled to large quantities and yields a disposable, simple-to-use device that allows for rapid detection of viruses.

1. Introduction

Viral diseases consistently rank as a leading cause of death worldwide.[1] Ability to control the spread of infections and minimize fatalities depends directly on the accuracy and speed of viral pathogen identification. For certain diseases, such as influenza, much effort has been devoted to the development of fast detection tools, such as rapid influenza diagnostic tests. These tests are based on viral nucleoprotein antigen recognition; and while they are rapid (usually taking less than 30 min), they lack sensitivity and the ability to distinguish between different viral strains.[2,3] Diagnosis of other viral diseases often relies solely on laboratory methods, such as virus isolation by cell culture or polymerase chain reaction (PCR) assays. These methods take far too long for real-time monitoring of pathogens and are costly and labor-intensive.[4–6] Thus, an urgent need exists for a general tool that can detect viral pathogens at the point of care, rapidly, selectively, and at low cost.[4,7] In this study, we have developed a method for producing robust nanopatterened polymer films that can rapidly and selectively capture and detect target viruses from a low-volume liquid sample without employing any flow-focusing or mass sensing devices. We adopted the principles of cell imprinting, which can be explained as a template-assisted assembly of functional groups on the surface of a polymer for recognition of structural and chemical features of target cells.[8–11] We employed nanometric viral templates to produce virus imprinted polymers (VIPs).

Previously, it was shown that virus-imprinted silica particles can selectively capture icosahedral plant viruses from 120 μL of aqueous sample with a viral concentration of 65 pM.[12] Rod-shaped plant virus was preferentially captured by imprinted crosslinked poly(allylamine hydrochloride) hydrogels, and this system reached a capture ratio of about 2 : 1 target to non-target plant virus.[13] A follow-up study showed an increased selectivity of an optimized imprinted poly(allylamine hydrochloride) toward the target virus (ratio about 7.8 : 1) when the polymer was immersed into 0.1 mg ml^{-1} suspension of either virus and centrifuged for 6 hours, and the conditions were further optimized.[14,15] Another study reported the formation of polymer-based acrylamide nanoparticles imprinted with waterborne bacteriophages and coupled to a surface plasmon resonance biosensor. This device was able to bind the bacteriophage from a 100 μL sample with viral concentrations of 0.33–27 pM.[16] Finally, much recent attention was devoted to coupling VIPs with quartz crystal microbalance (QCM) sensors for high sensitivity and selectivity.[17–19] Imprinted acrylamide polymers spin-coated on QCM electrodes were able to distinguish between different subtypes of Influenza A. Typical experiments were conducted by flowing 75 μL of viral suspension at a concentration of 2 × 10^7 particles per mL (33 fM) through the QCM cell, while the absolute limit of measure-

[a]*Department of Chemistry, Stanford University, Stanford, California 94305-5080, USA. E-mail: zare@stanford.edu*
[b]*Department of Chemistry, Hong Kong Baptist University, Waterloo Road, Hong Kong, P. R. China*
[c]*Gray Box Biology LLC, New York, New York 10027, USA*

ment was about 10^5 particles per mL (0.17 fM).[18] Although coupling virus imprinting with the QCM enables high sensitivity, it also relies on accessibility of the microbalance and often requires sophisticated polymer preparation to ensure that the imprinting material is rigid enough to maintain the quality factor of resonance.

In our study, a low-cost tool for selective viral detection was developed without employing any mass sensing or flow-focusing devices. Polydimethylsiloxane (PDMS), an inexpensive, commercially available polymer, served as the thin film for imprinting and enabled rapid capture of viral pathogens in minute sample volumes.[9] We employed as model pathogens Influenza A H3N2 (HK68), which was responsible for the 1968–1969 pandemic flu outbreak, and a morphologically similar virus strain, Newcastle Disease Virus (NDV).[20] For safety reasons, both strains were inactivated prior to use.

2. Experimental

2.1 Materials

UV-inactivated HK68 particles and UV-inactivated NDV particles (two batches each: unlabeled virus and virus labeled with DiO, 3,3′-dioctadecyloxacarbocyanine perchlorate) were obtained from Gray Box Biology LLC, (New York, NY). Polydimethylsiloxane (PDMS) was obtained from Momentive Performance Materials, Dowd & Guild (San Ramon, CA). All other chemicals were purchased in analytical or higher grade from Sigma-Aldrich (St. Louis, MO) or VWR International (Visalia, CA).

2.2 Confirmation of virus particle size and concentration

Prior to experimentation it was necessary to establish a framework for consistently measuring the interactions between the VIP and the two types of virus particles. Viral titers are traditionally determined using plaque-based assays, and reported as plaque forming units per ml (pfu ml^{-1}). However, for this study, it was preferable to express the concentrations in terms of free particles per mL. The concentrations of HK68 and NDV suspensions, respectively, were normalized to particles per mL and later to molarities *via* dynamic light scattering (DLS) using a Nano-ZS90 Zetasizer (Malvern, UK). For the purposes of this study, we established that 1 pfu of NDV is equivalent to approximately 6.7 particles. The sizes of HK68 and NDV particles were also confirmed *via* DLS. All measurements were made in triplicate.

2.3 Calibration of fluorescence intensities

A calibration curve was built to relate fluorescence intensities produced by DiO-labeled HK68 and NDV to virus concentrations. This step is crucial because we measured virus capture *via* fluorescence microscopy (iXon+ electron-multiplying CCD camera at linear mode from Andor Technology, U.K. and Andor Solis imaging software) and must account for the possibility that the two viral strains have different fluorescence yields. We confirmed that fluorescence intensities correlate with virus concentration and exhibit linearity at concentrations in the range of 10^6–10^9 particles per mL.

2.4 Characterization of HK68

HK68 virus suspension was imaged using transmission electron microscopy (TEM) with a JEM-1400 TEM (Jeol, Japan) at 120 kV and a Gatan Orius digital camera. Prior to imaging, the suspension was contrast-stained for 15 min with an aqueous solution of uranyl acetate 1 wt%. Formvar- and carbon-coated copper glow discharged grids (300–400 mesh) were used.

2.5 Template preparation

A 2 μL suspension of the UV-inactivated HK68 virus particles (approximately 10^9 particles per mL) was applied to the surfaces of precleaned polystyrene microscope slides and kept at 60 °C for 2 h. The locations of the virus smears were labeled with a permanent marker; excess material on the surfaces was removed by rinsing the substrate with DI water. The substrate was dried at 60 °C for 10 min before being used as a template. The NDV template is prepared in a similar manner.

2.6 Stamp fabrication[11]

We have developed this nanopatterning procedure based on the polymer imprinting protocol developed in our previous work.[8] In short, we weighed the PDMS monomer and cross-linker (curing agent) in a 10 : 1 ratio and mixed them manually. This mixture was then degassed in a vacuum desiccator until no bubbles were visible and was subsequently cured in an 80 °C oven for 30 min. Once the PDMS hardened, it was cut into squares with a side length of about 0.5 inch. These squares served as the base for the thin film used for imprinting. The thin film was prepared by diluting the PDMS curing mixture using cyclohexane in a 2 : 1 ratio. This solution was spincoated onto the square base (30 s at 1500 rpm, using WS-650-23 Spin Coater, Laurell Technologies, PA). While stamp fabrication conventionally uses glass as the base for the imprinted polymer, we chose to use PDMS as the base and thin film because of its flexibility and ease of preparation. Both the template and PDMS prepolymer were exposed to 60 °C for 15 min, after which the template stamp was pressed into the prepolymer and left to cure at 37 °C for 24 h. The template was then removed, and any remaining virus particles were washed away with an excess of water. The VIP was characterized *via* atomic force microscopy (AFM) with a scanning probe microscope (XE-70, Park Systems, CA) under noncontact AFM (tapping) mode, using etched silicon cantilevers (resonance frequency ~300 kHz, with medium low tip oscillation damping ~15%) and a scan rate of 0.2 Hz and XEI software. AFM images were analyzed with ImageJ software (National Institutes of Health).

2.7 Virus capture

The imprinted surface was tested for its ability to selectively reincorporate the target virus, which was labeled with DiO for detection purposes. The HK68 suspension was diluted with DI water in a 1 : 20 ratio (approximately 5×10^7 particles per mL).

The virus suspension was applied by simply dropping an ultra-low volume of the suspension (5 μL) onto the imprinted surface of the polymer using a micropipette. After 15 min of static exposure, the imprinted polymer was rinsed with DI water to ensure that unattached virus particles were removed. The imprinted surface of the polymer was then inspected with fluorescence microscopy.

2.8 Exposure time

The effect of time of exposure to the target virus on virus capture was tested following the procedure in the section 2.7. Exposure times tested were 1 min, 2 min, 3 min, 4 min, 5 min, 10 min, 20 min, 45 min, 1 h, and 2 h.

2.9 Sensitivity

The suspension with the target virus was progressively diluted with DI water. The most dilute suspension was 1 : 200. Imprinted polymers were exposed to 5 μL of the diluted suspensions for 20 min.

2.10 Selectivity

Imprinted polymers produced with HK68 were exposed to an undiluted suspension of DiO-labeled NDV (approximately 6.7×10^7 particles per mL) for 1, 5, and 20 min; conversely, imprinted polymers produced with NDV were exposed to an undiluted suspension of DiO-labeled HK68 (1×10^9 particles per mL) for the same time intervals.

3. Results and discussion

3.1. Characterization of viral suspensions

We first characterized the HK68 virus suspension *via* TEM and observed spherical morphology with typical glycoprotein spikes protruding from the particle surface (Fig. 1). DLS measurements of both strains confirmed the size of HK68 as 119 ± 52 nm and the size of NDV as 176 ± 16 nm, in line with literature on virus morphology, while the larger size distribution range observed for HK68 may suggest some aggregation.[18,21–25]

3.2. Polymer film nanopatterning

VIPs were successfully produced from PDMS thin films based on the optimized protocol using viruses as nanometric imprinting templates (Fig. 2).[9] The template containing the target virus was pressed into a PDMS prepolymer; and after the polymer cured, the template and excess virus particles were removed, leaving behind in the polymer cavities complementary in shape and exhibiting a specific affinity for the target virus.

HK68 was the first target virus used in nanopatterning. AFM images confirmed the presence of nanometric cavities complementary to the shape of the virus on the PDMS film, with good surface coverage (Fig. 3). The mean size of the

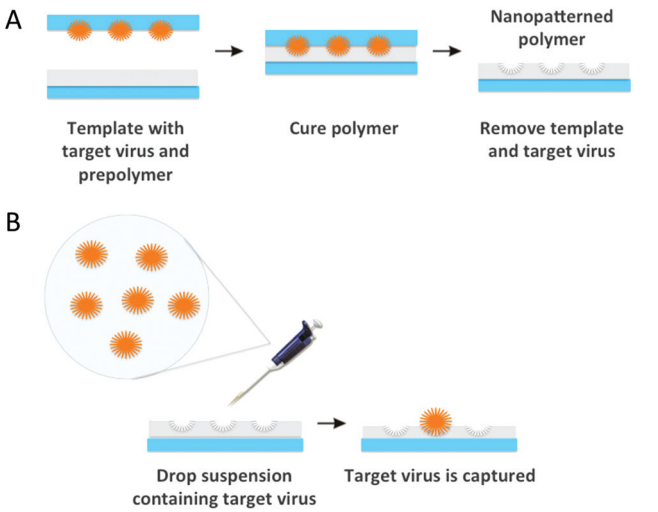

Fig. 2 Schematic representation of PDMS film nanopatterning with viruses showing (A) production and (B) capture.

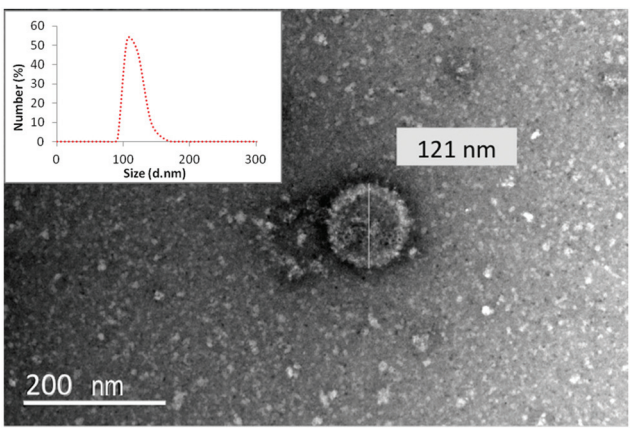

Fig. 1 TEM image of HK68 virus particle with spherical morphology. The inset presents a typical DLS measurement.

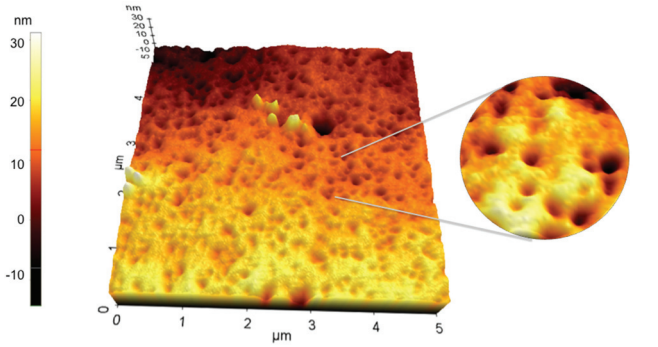

Fig. 3 AFM images of PDMS surface nanopatterned with HK68 (target virus). The insert is at a magnification of 4×.

cavities was 120 ± 4 nm, while their maximum and minimum dimensions were 320 nm and 47 nm, respectively. The polymer surface seemed to be patterned by a monolayer of virus particles, although about one in every twenty cavities was deeper. It is noteworthy that UV-inactivated HK68 virus was used for the imprinting process, obviating the use of hazardous live pathogens in large-scale production of VIPs.[4]

3.3. Virus capture

Virus capture was tested using DiO-labeled virus samples to facilitate identification by a fluorescence microscope. Fluorescence intensity of 2000 counts was recorded after only 1 minute of exposing the VIP to 5 μL of virus sample. This signal was about ten times higher than that of the control (nonimprinted PDMS film exposed to the same virus sample), indicating the presence of DiO-labeled viruses captured in the cavities of the polymer.

We investigated the influence of exposing the VIP to the virus sample for various time intervals. We found that VIPs were effective in capturing the target virus with only 1 min of exposure and that fluorescence intensity values steadily increased with time before plateauing at about 45 min of exposure (Fig. 4).

The results suggest that while detection is possible almost immediately, the optimal time of static exposure would be around 20 min. Exposing the VIP to any virus for longer than 20 min would increase the chance of nonspecific interaction of particles and would not satisfy clinical needs of efficiency.[2] In terms of real-time disease monitoring, the VIP presents a significant improvement on the laboratory gold standard method for the specific detection of Influenza A: rRT-PCR assay, which takes about 2.5 h.[26]

Having thus established 20 min as the optimal time of exposure, we identified the lowest concentrations threshold for virus capture. The minimal virus capture perceivable by fluorescence microscopy was at the virus concentration of 8 fM in a 5 μL sample. This virus concentration is within the range physiologically found in saliva or nasal washes of subjects infected with Influenza A.[27] In addition, the ultralow volume of the sample required for the analysis enables reaching several orders of magnitude higher sensitivity by simply preconcentrating the specimen. Preconcentration by moisture evaporation is feasible under field conditions and should take no more than a few minutes.

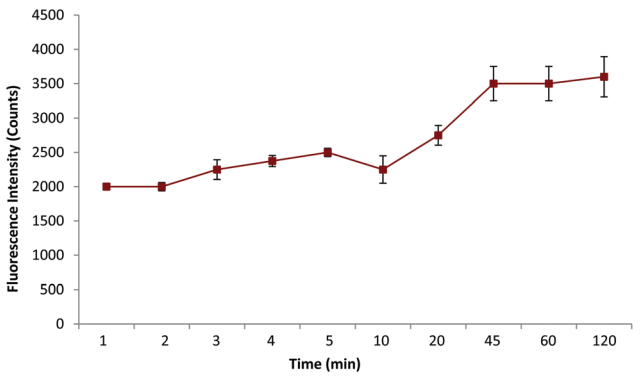

Fig. 4 Change in virus capture across various times of exposure. Error bars represent one standard deviation of three fluorescent measurements.

In the present study, virus capture is achieved using only static exposure to a virus suspension. It is anticipated that the sensitivity might be further improved by increasing the contact of virus particles with the imprinted surface, such as using flow or other means, like centrifugation, to press the virus particles against the VIP. It is noteworthy that fluorescence is just one means of detecting the captured virus. Virus particles already incorporated into cavities on the polymer can be visualized by staining with dyes specific to viral coat proteins or attaching fluorescent antibodies. Both of these procedures can be performed easily in field conditions. Thus, it is envisioned that VIP platforms can be designed to work in the field without the availability of electricity and to meet the World Health Organization guidelines.[28]

3.4 Selectivity

We confirmed the ability of the VIP to capture only the target virus by exposing the VIP imprinted with HK68 to a concentrated sample of NDV and *vice versa*. The two viruses have a similar shape (spherical morphology, although pleomorphism can occur) and size, but differ in their surface components. Glycoproteins protrude from the surface of both viruses but with different densities.[21–25] The surface of HK68 is covered primarily with hemagglutinin and neuraminidase glycoproteins, while the surface of NDV contains the fusion glycoprotein and hemagglutinin-neuraminidase glycoprotein.[29,30] The difference in surface composition accounts for the ability of the VIP to distinguish between the two viruses. The PDMS kit utilized in VIP production contains a mixture of PDMS oligomers with vinyl groups, cross-linkers of polysiloxanes with vinyl and hydrogen groups, and a low amount of additional components including octamethylcyclotetrasiloxane, benzene, toluene and ethylbenzene.[10] All these ingredients contain functional groups that can form specific interactions with the template virus during the curing process and assume the most thermodynamically favorable orientation for these specific interactions. As the polymer is further cured, the position of the functional groups in the nanopatterned region becomes fixed. The virus particle template is removed, but the resultant cavity continues to select the target virus. We observed that the polymer film, which was first nanopatterned with HK68 and exposed sequentially to suspensions containing fluorescently labeled NDV and HK68, was able to preferentially capture HK68 after just 1 min at a capture ratio of about 1 : 6.7 ± 0.5 (Fig. 5). A capture ratio of 1 : 8.0 ± 1.0 was obtained after 20 min, which was previously established as the optimal exposure time (Fig. 5). When the nanopatterning protocol was reversed and the VIP was imprinted with NDV, the ratio of capture of HK68 to NDV was 1 : 7.6 ± 0.7 with 20 min. It is reasonable to assume that, because NDV particles are slightly larger than HK68 particles, it is somewhat easier for HK68

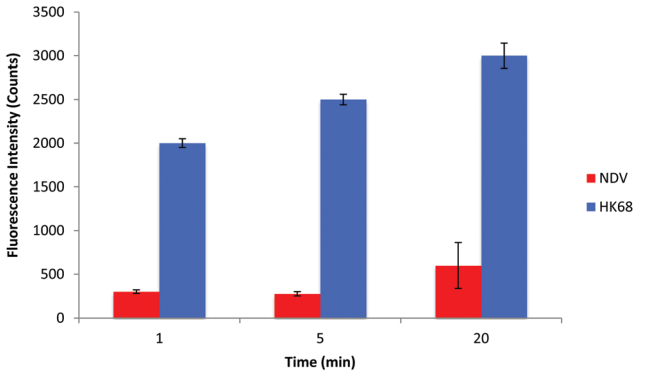

Fig. 5 Sample virus capture measurement by fluorescence intensity. Error bars represent one standard deviation of three fluorescence measurements. Note that the virus capture ratio is calculated from multiple experiments according to calibration curves that account for the difference in concentration between the two strains.

particles to be nonspecifically incorporated into the VIP produced for NDV due to the Brownian motion.[17,18] Nevertheless, the high selectivity ratio of the VIP is maintained. This offers further evidence that chemically specific recognition of the virus by the imprinted surface of the VIP is the dominant mechanism for virus capture as opposed to simple physical shape selection.[10]

We acknowledge that biological samples such as saliva are more complex than those used in this study. Future work will be conducted with saliva samples obtained from a statistically significant number of individuals to confirm selectivity in physiological fluids.

4. Conclusions

We have found that PDMS thin films can be successfully imprinted with viruses, creating nanometric cavities on the polymer surface. These cavities, which are complementary in size and shape to the template virus, enable selective detection of the virus in suspension. We suggest that virus imprinted polymers (VIPs) may have distinct advantages over other alternatives for viral detection based on their ability to capture selectively viruses from ultralow volumes of liquid samples (5 μL), their good sensitivity achieved without any mass sensing or flow-focusing devices (virus detection limit of 8 fM), and their rapid response (1 min). Furthermore, the excellent ability of the VIPs to distinguish between two virus strains similar in size and shape offers evidence for the feasibility of using VIPs as a point-of-care diagnostic tool. The imprinting protocol developed for the two viral strains, HK68 and NDV, can likely be generalized and adapted to other enveloped viral strains.

Conflict of interest

The authors declare no competing financial interest.

Acknowledgements

The authors thank John Perrino at the Cells Science Imaging Facility at Stanford University for help in preparing the TEM images. K.M. is grateful to Yad Hanadiv – the Rothschild Foundation and to the Center for Molecular Analysis and Design at Stanford for their support of the author's postdoctoral research. This work was supported by the Stanford SPARK program.

References

1 Fact sheet No. 310, World Health Organization 2014, http://www.who.int/mediacentre/factsheets/fs310/en/, (accessed August 2014).
2 WHO Recommendations on the Use of Rapid Testing for Influenza Diagnosis, World Health Organization 2005, http://www.who.int/influenza/resources/documents/RapidTestInfluenza_WebVersion.pdf, (accessed August 2014).
3 *Guidelines for Clinicians on the Use of Rapid Influenza Diagnostic Tests*, Center for Disease Control and Prevention 2014, http://www.cdc.gov/flu/professionals/diagnosis/clinician_guidance_ridt.htm, (accessed December 2014).
4 S. Sykora, A. Cumbo, G. Belliot, P. Pothier, C. Arnal, Y. Dudal, P. F. Corvini and P. Shahgaldian, *Chem. Commun.*, 2015, **51**, 2256–2258.
5 G. M. Birnbaumer, P. A. Lieberzeit, L. Richter, R. Shirhagl, M. Milnera, F. L. Dickert, A. Bailey and P. Ertl, *Lab Chip*, 2009, **9**, 3549–3556.
6 N. F. Walker, C. S. Brown, D. Youkee, P. Baker, N. Williams, A. Kalawa, K. Russell, A. F. Samba, N. Bentley, F. Koroma, M. B. King, B. E. Parker, M. Thompson, T. Boyles, B. Healey, B. Kargbo, D. Bash-Taqi, A. J. Simpson, A. Kamara, T. B. Kamara, M. Lado, O. Johnson and T. Brooks, *Euro Surveill.*, 2015, **20**, 21073–21078.
7 G. A. Storch, *Clin. Infect. Dis.*, 2000, **31**, 739–751.
8 R. Schirhagl, E. W. Hall, I. Fuereder and R. N. Zare, *Analyst*, 2012, **137**, 1495–1499.
9 K. Ren, N. Banaei and R. N. Zare, *ACS Nano*, 2013, **7**, 6013–6036.
10 K. Ren and R. N. Zare, *ACS Nano*, 2012, **6**, 4314–4318.
11 R. Schirhagl, K. Ren and R. N. Zare, *Sci. China: Chem.*, 2012, **55**, 1–15.
12 A. Cumbo, B. Lorber, P. F. X. Corvini, W. Meier and P. Shahgaldian, *Nat. Commun.*, 2013, **4**, 1503.
13 L. D. Bolisay, J. N. Culver and P. Kofinas, *Biomaterials*, 2006, **27**, 4165–4168.
14 L. D. Bolisay, J. N. Culver and P. Kofinas, *Biomacromolecules*, 2007, **8**, 3893–3899.
15 L. D. Bolisay and P. Kofinas, *Macromol. Symp.*, 2010, **291–292**, 302–306.
16 Z. Altintas, M. Gittens, A. Guerreiro, K. A. Thompson, J. Walker, S. Piletsky and I. E. Tothill, *Anal. Chem.*, 2015, **87**, 6801–6807.

17 M. Jenik, R. Schirhagl, C. Schirk, O. Hayden, P. Lieberzeit, D. Blaas, G. Paul and F. L. Dickert, *Anal. Chem.*, 2009, **81**, 5320–5326.
18 T. Wangchareansak, A. Thitithanyanont, D. Chuakheaw, M. P. Gleeson, P. A. Lieberzeit and C. Sangma, *J. Mater. Chem. B*, 2013, **1**, 2190–2197.
19 F. L. Dickert, O. Hayden, R. Bindeus, K. J. Mann, D. Blaas and E. Waigmann, *Anal. Bioanal. Chem.*, 2004, **378**, 1929–1934.
20 C. Viboud, R. F. Grais, B. A. P. Lafont, M. A. Miller and L. Simonsen, *J. Infect. Dis.*, 2005, **192**, 233–248.
21 S. V. Bourmakina and A. Sastre-García, *J. Gen. Virol.*, 2003, **84**, 517–527.
22 J. Seladi-Schulman, J. Steel and A. C. Lowen, *J. Virol.*, 2013, **87**, 13343–13353.
23 H. Garoff, R. Hewson and D. E. Opstelten, *Microbiol. Mol. Biol. Rev.*, 1998, **62**, 1171–1190.
24 P. C. Roberts and R. W. Compans, *Proc. Natl. Acad. Sci. U. S. A.*, 1998, **95**, 5746–5751.
25 T. A. Bowden and E. E. Fry, in *Functional and Structural Proteomics of Glycoproteins*, ed. R. Owens and J. Nettleship, Springer, Berlin, 2011, vol. 7, pp. 159–180.
26 X. Xu, H. Bao, Y. Ma, J. Sun, Y. Zhao, Y. Wang, J. Shi, X. Zeng, Y. Li, X. Wang and H. Chen, *Virol. J.*, 2015, **12**, 69–74.
27 M. Nicas and R. M. Jones, *Risk Anal.*, 2009, **29**, 1292–1303.
28 X. Mao and T. J. Huang, *Lab Chip*, 2012, **12**, 1412–1416.
29 X. Cheng, J. R. Zendel, Q. Xu and H. Jin, *Virology*, 2012, **432**, 91–98.
30 Z. Huang, A. Panda, S. Elankumaran, D. Govindarajan, D. D. Rockemann and S. K. Samal, *J. Virol.*, 2004, **78**, 4176–4184.